

1                                    **Electronic Supplementary Information for:**  
2                                    **Deformability of Mg-Aluminosilicate glass under High Pressure and**  
3                                    **Shear Stress: Dynamic Coordination Change of Al<sup>3+</sup>**

4  
5                                    Kosei Osada<sup>a</sup>, Akihiro Yamada<sup>a, b</sup>, Koji Ohara<sup>c</sup>, Satoshi Yoshida<sup>a, b</sup> and Jun Matsuoka<sup>a, b</sup>

6  
7                                    a) Department of Materials Chemistry, The University of Shiga Prefecture,  
8                                    Hassaka-cho, Hikone, Shiga 522-8533, Japan

9                                    b) Center for Glass Science and Technology, The University of Shiga Prefecture,  
10                                    Hassaka-cho, Hikone, Shiga 522-8533, Japan

11                                    c) Diffraction and Scattering Division, Japan Synchrotron Radiation Research Institute (JASRI),  
12                                    Sayo-gun, Hyogo, 679-5198, Japan.

13  
14                                    Corresponding author: Akihiro Yamada,  
15                                    Email: yamada.ak@mat.usp.ac.jp

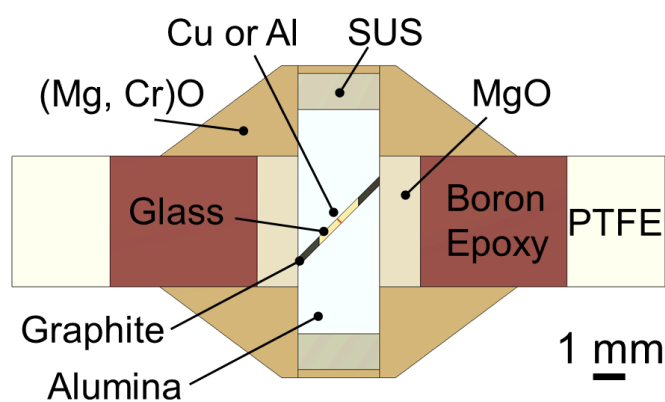
16

17 **Pressure-cell setup of the high-pressure deformation experiment**

18 The glass sample, prepared as described above, was positioned at the center of the high-pressure cell  
19 shown in Fig. S1. To apply a simple shear stress, the sample was sandwiched between a pair of 45°-  
20 cut alumina pistons. Along the compression axis, SUS303 stainless steel and (Mg,Cr)O were used as  
21 backing materials, and the applied shear stress was controlled by varying the thickness of these  
22 components. The sample was enclosed by a graphite ring, and the entire assembly of sample and  
23 pistons was surrounded by an MgO sleeve. This assembly was then placed inside a boron-epoxy  
24 pressure medium, which was supported by an outer PTFE ring to prevent collapse during loading.

25

26



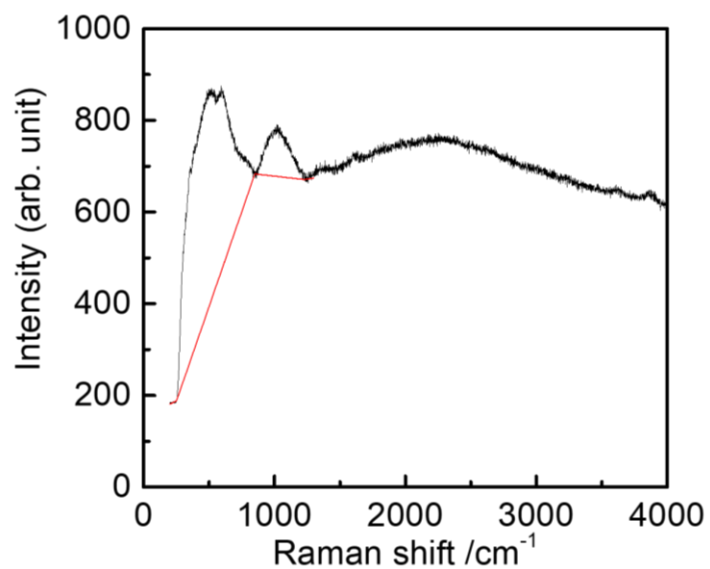
27

28 Fig. S1. A cross section of the cell assembly used in the deformation experiment of the modified  
29 Paris-Edinburgh anvils system. The compression axis is vertical axis (see ref: 15 on the detail  
30 of the compression geometry).

31 **Baseline subtraction of Raman Spectroscopy**

32 The spectra of the deformed samples exhibited a background, which was corrected by baseline  
33 subtraction, as illustrated in Fig. S2.

34

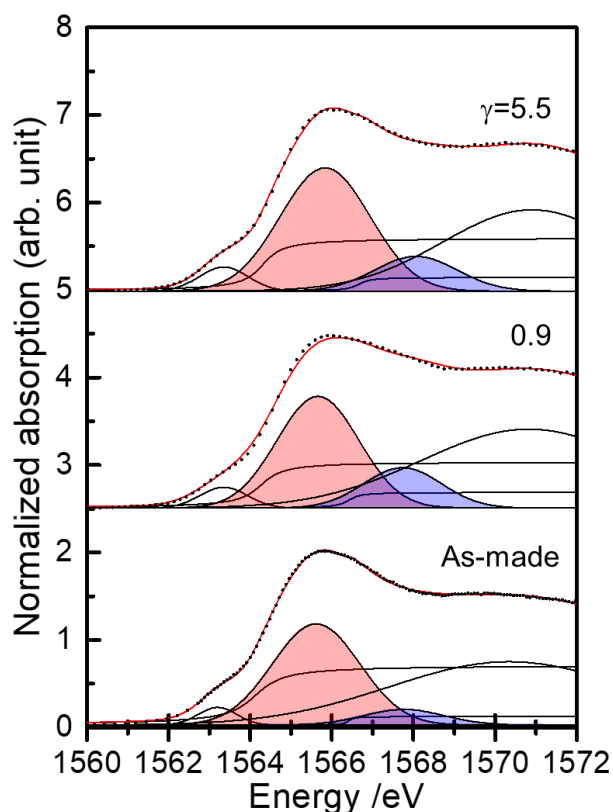


35

36 Fig.S2 Example for the background correction in Raman spectra. Black line and red line indicate  
37 Raman spectra and baseline, respectively. Region at 0-1300 cm<sup>-1</sup> is spectrum of glass, and  
38 1300-4000 cm<sup>-1</sup> is background.

39 **Al coordination number estimation from Al K-edge XANES**

40 To quantify the aluminum coordination states, XANES spectra were deconvoluted following  
 41 previous studies.<sup>16,17</sup> The results of the analysis are shown in Fig. S3 and Table S1. Note that this  
 42 analysis only considers two aluminum coordination states, <sup>[IV]</sup>Al and <sup>[VI]</sup>Al, to avoid over-  
 43 parameterization.



45  
 46 Fig.S3 Al K-edge X ray absorption spectra of as-made and deformed glasses. Dotted lines represent  
 47 the experimental spectra. Black and red lines correspond to the deconvolution results and the  
 48 synthesized spectra, respectively. The hatched red and blue components indicate  
 49 contributions from <sup>[IV]</sup>Al and <sup>[VI]</sup>Al, respectively.

51 Table S1 Fitting parameters of deconvoluted peaks in XANES spectra of the glasses

Shear strain, $\gamma$	AlO <sub>4</sub>			AlO <sub>6</sub>			Third peak		
	Position /eV	FWHM /eV	Area	Position /eV	FWHM /eV	Area	Position /eV	FWHM /eV	Area
0	1565.6	2.5	3.1	1567.8	2.3	0.4	1570.3	6.9	5.3
0.92	1565.7	2.4	3.2	1567.7	2.2	1.1	1570.8	6.2	5.9
3.94	1565.7	2.5	3.6	1567.7	2.4	0.6	1570.6	5.5	4.7
4.80	1565.7	2.5	3.4	1567.9	2.3	0.9	1570.7	4.9	3.8
5.46	1565.8	2.6	3.9	1568.1	2.4	1.0	1570.9	5.1	5.1

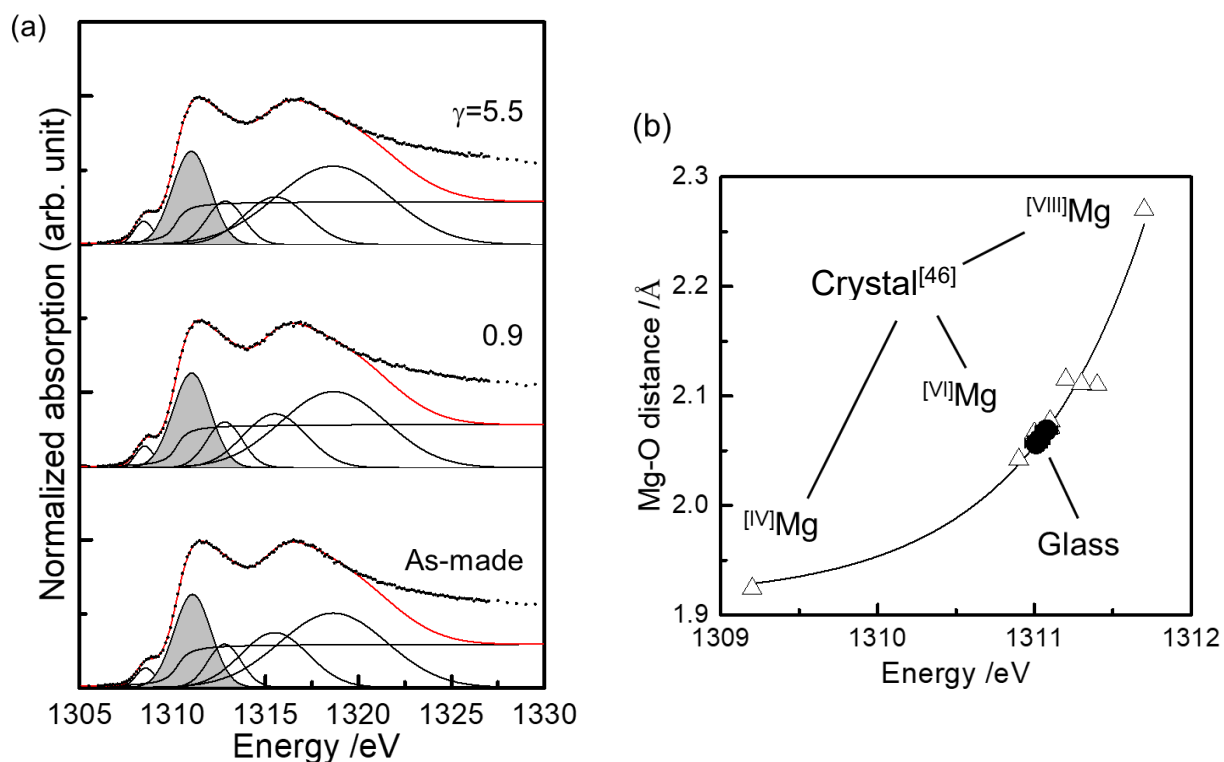
52  
 53

54 **Mg K-edge X-ray Absorption Near-Edge Spectroscopy (XANES)**

55 Mg K-edge XANES measurements were performed at the BL-13 beamline of the Ritsumeikan  
56 University SR Center. White synchrotron radiation was monochromatized using a KTP(011) crystal  
57 and directed onto the sample surface. The spectra were collected over an energy range of 1250–1350  
58 eV in fluorescence yield mode, using a Silicon Drift Detector (SDD) positioned at 90° to the incident  
59 beam. The energy scale was calibrated by setting the K-edge peak of a reference MgO sample to 1311.3  
60 eV. The collected spectra were then deconvoluted using a Gaussian function and an arctangent step-  
61 function. The raw spectrum and the result of this deconvolution are shown in Fig. S4a.

62 The position of the deconvoluted Mg K-edge peak has been reported to correlate with the  
63 magnesium-oxygen bond distance.<sup>54</sup> The peak position observed in our samples corresponds to that of  
64 six-fold coordinated Mg (Fig. S4b). Although the peak position shifted slightly to a lower energy with  
65 increasing strain, the total shift was less than 0.1 eV. This corresponds to an estimated change in bond  
66 distance of only ~0.01 Å. Therefore, it is concluded that no significant change in the Mg coordination  
67 number occurred as a result of the deformation.

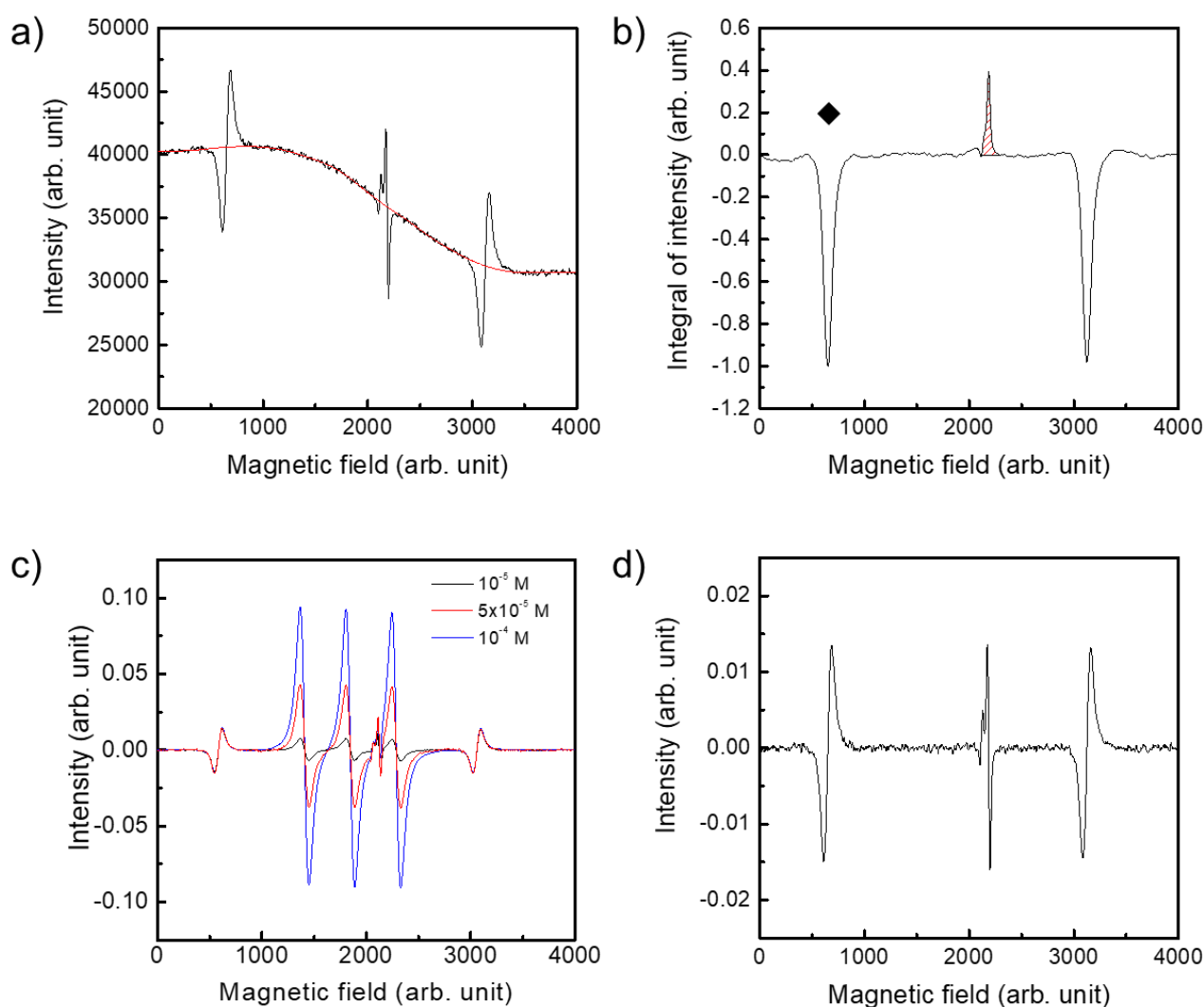
68



69 Fig. S4 (a) Mg K-edge XANES spectra of MAS glasses. Solid dots indicate XANES spectrum. Black  
70 and red lines show deconvoluted peaks and sum of ones. Gray hatch indicates peak A. (b)  
71 Calibration curve for Mg-O distance from Ref: 46 (triangles). Solid symbols are this work.  
72

73 **Determination of Defect Concentration by Electron Spin Resonance Spectroscopy**

74 Baseline correction was applied to the raw spectra (Fig. S5a), and the intensity profiles were  
75 subsequently integrated and normalized to the  $\text{Mn}^{2+}/\text{MgO}$  peak (Fig. S5b, diamond) prior to calculating  
76 spin concentrations. Spin concentrations were determined from the double integration of the signal  
77 (Fig. S5b, red hatch). A calibration curve for spin concentration was obtained using solutions of  
78 TEMPOL (4-hydroxy-2,2,6,6-tetramethylpiperidin-1-oxyl) in dehydrated benzene at different  
79 concentrations. Examples of baseline-corrected ESR profiles of TEMPOL and the glass are shown in  
80 Fig. S5c and S5d, respectively.



81  
82 Fig. S5 (a) Raw ESR signal (black line) and baseline (red line) for the glass sample. (b) Integrated  
83 profile of the glass after baseline correction and intensity normalization. The red hatch and diamond  
84 indicate the double integration of the sample ESR signal and the  $\text{Mn}^{2+}/\text{MgO}$  peak, respectively. (c)  
85 Examples of ESR signals of TEMPOL after baseline correction and intensity normalization. (d) An  
86 example of the ESR signal of the glass sample after baseline correction and intensity normalization.